

## PULSATILE FLOW OF BLOOD IN MILD STENOSIS: EFFECTS OF BODY ACCELERATION

N.K. Verma, S.U. Siddiqui, R.S. Gupta\*

Department of Mathematics, Harcourt Butler Technological Institute, Kanpur- 208002, India  
\*Department of Applied Sciences, Kamla Nehru Institute of Technology, Sultanpur, India

### Abstract

This article is concerned with the analysis of pulsatile flow of blood through a stenosed artery including the effects of external body acceleration. The pulsatile flow behavior of blood in an artery under stenotic conditions subject to the pulsatile pressure gradient and external body acceleration has been studied. The effects of pulsatility, stenosis, body acceleration, yield stress and impedance have been investigated by modeling blood as a Casson fluid. It is observed that the yield stress of the fluid and body acceleration highly influenced the velocity of the fluid, shear stress, flow rate and impedance in a stenosed artery. It is interesting to note that the body acceleration enhances the flow rate and reduces the impedance.

**Keywords:** Body acceleration, Casson fluid, Stenosis, Yield stress, Impedance, Pulsatile.

### INTRODUCTION

Blood flow under normal physiologic conditions is an important field of study, as is blood flow under diseased conditions. The majority of deaths in developed countries result from cardiovascular diseases, most of which are associated with some form of abnormal blood flow in arteries. Blood flow and pressure are unsteady. The cyclic nature of heart pump creates pulsatile conditions in all arteries. The heart ejects and fills with blood in alternating cycles called *systole* and *diastole*. Blood is pumped out of the heart during systole. The heart rests during diastole, and no blood is ejected. Pressure and flow have characteristic pulsatile shapes that vary in different parts of arterial system. In order to understand the blood flow behavior in arteries so as to provide sufficient information for clinical purposes, intensive research has been carried out worldwide for both normal and stenotic arteries [17, 18, 19, 22, 23, 28]. Most analysis assumed the human blood to be Newtonian and the stenosis to be symmetric to make the problem more traceable [12, 13]. Various mathematical models have been developed to simulate blood flow through the stenotic arteries, including Newtonian and non-Newtonian models [8, 9, 10, 29]. To understand the effects of a single mild stenosis present in the arterial lumen, a good number of studies [6, 11, 20, 30, 31, 32] on the blood flow through stenosed arteries have been performed. All these studies were made with the assumption that the flowing blood is Newtonian and the geometry of the stenosis is a smooth cosine function.

Due to physiological importance of body acceleration many theoretical investigations have been carried out for the flow of blood under the influence of body acceleration with and without stenosis. Sud and Sekhon [21] studied the pulsatile flow of blood through a rigid circular tube subject to body acceleration, treating blood as Newtonian fluid. Mishra and Sahu [21] analyzed the flow of blood through large arteries under the action of periodic body acceleration. Belardinelli et. al. [1] proposed

mathematical models for various forms of body accelerations. Using Laplace and Hankel transforms Elshehawey et. al. [5] studied the effect of body acceleration on pulsatile flow of blood through a porous medium by treating blood as a Newtonian fluid. Later El-Shahed [4] extended this study for a stenosed porous medium.

In all these investigations blood is modeled as a Newtonian fluid. It is well established that blood being a suspension of corpuscles behaves like a non-Newtonian fluid [2, 7, 20] in small diameter tubes. Experiments conducted on blood [3, 16, 26] suggested that the behaviour of blood at low shear rates can be described by Casson model. Majhi and Nair [14] studied the pulsatile flow of blood under the influence of body acceleration treating blood as a third grade fluid. Flow of a Casson fluid in a tube filled with porous medium under periodic body acceleration with applications to artificial organs [24]. Recently a two dimensional mathematical model has been developed to study the effect of externally imposed periodic body acceleration on non-Newtonian flow of blood through an elastic stenosed artery where the blood is characterized by power-law model [15].

In view of the above, an attempt is made in the present theoretical investigation to evaluate some of the important characteristics of blood flow past an arterial stenosis constrained with the pulsatile pressure gradient and a cycle of body acceleration. Blood is modeled as a Casson fluid. Effects of pulsatile nature of blood including the stenosis, body acceleration yield stress on flow parameters are shown graphically. The yield stress and body acceleration highly influenced the velocity of blood, shear stress, flow rate and impedance.

## FORMULATION OF THE PROBLEM

Let us consider a one-dimensional pulsatile flow of blood in an artery with mild stenosis by considering blood as a Casson fluid. The flow is considered as axially symmetric, pulsatile and fully developed. The geometry of the flow is shown in Figure 1.

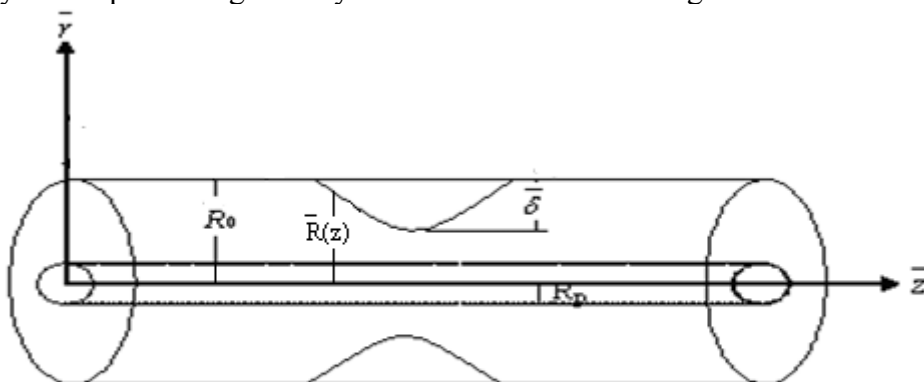


**Fig.1. Geometry of stenosed artery**

Consider a bell-shaped stenosis geometry given by

$$\frac{\bar{R}(\bar{z})}{R_0} = 1 - \frac{\bar{\delta}}{R_0} \exp\left(-\frac{m^2 \varepsilon^2 \bar{z}^2}{R_0^2}\right) \quad (1)$$

where  $R_0$  is the radius of the arterial segment outside the stenosis,  $\bar{R}(\bar{z})$  is the radius of the stenosed portion of the arterial segment under consideration,  $\bar{z}$  is the axial

coordinate,  $\bar{\delta}$  is the maximum height of the stenosis at the throat and  $m$  is a parametric constant,  $\varepsilon$  denotes the relative length of the constriction (*i.e.*  $\varepsilon = R_0/L_0$ ). The periodic body acceleration  $F(\bar{t})$  in the axial direction is given by

$$F(\bar{t}) = a_0 \cos(\omega_b \bar{t} + \varphi) \quad (2)$$

where  $a_0$  is the amplitude,  $\omega_b = 2\pi f_b$ ,  $f_b$  is the frequency in Hz,  $\varphi$  the lead angle of  $F(\bar{t})$ . The frequency of body acceleration  $f_b$  is assumed to be small, so that wave effects can be neglected. This pressure gradient at any  $\bar{z}$  may be represent as follows

$$-\frac{\partial \bar{p}}{\partial \bar{z}} = A_0 + A_1 \cos(\omega_p \bar{t}), \quad (3)$$

where  $A_0$  is steady component of the pressure gradient,  $A_1$  is amplitude of the fluctuating component and  $\omega_b = 2\pi f_b$ ,  $f_b$  is the pulse frequency. Both  $A_0$  and  $A_1$  are function of  $\bar{z}$ . The equations governing the flow are

$$\bar{\rho} \frac{\partial \bar{u}}{\partial \bar{t}} = -\frac{\partial \bar{p}}{\partial \bar{z}} + \frac{1}{r} \frac{\partial}{\partial r} (\bar{r} \tau_{\bar{r}, \bar{z}}) + F(\bar{t}) \quad (4)$$

$$\frac{\partial \bar{p}}{\partial \bar{r}} = 0 \quad (5)$$

where  $\bar{r}, \bar{z}$  denote the radial and axial coordinates respectively and  $\bar{\rho}$  denote density,  $\bar{u}$  axial velocity of blood,  $\bar{t}$  time,  $\bar{p}$  pressure and  $\bar{\tau}$  the shear stress. Casson fluid relation between shear stress and shear rate is given by

$$\left. \begin{aligned} \bar{\tau}^{\frac{1}{2}} &= \bar{\tau}_y^{\frac{1}{2}} + \left[ \mu \left( -\frac{\partial \bar{u}}{\partial \bar{r}} \right) \right]^{\frac{1}{2}}, & \text{if } \bar{\tau} \geq \bar{\tau}_y \\ \frac{\partial \bar{u}}{\partial \bar{r}} &= 0 & \text{if } \bar{\tau} \leq \bar{\tau}_y \end{aligned} \right\} \quad (6)$$

where  $\bar{\tau}_y$  denote yield stress and  $\mu$  the viscosity of blood.

The boundary conditions are

$$\bar{u} = 0 \quad \text{at} \quad \bar{r} = \bar{R}(\bar{z}) \quad (7)$$

$$\bar{\tau} \text{ is finite at } \bar{r} = 0 \quad (8)$$

Conditions (7) and (8) are the standard no slip conditions at the artery wall.  
Introducing non-dimensional variables

$$\left. \begin{aligned} u &= \frac{\bar{u}}{A_0 R_0^2 / 4\mu}, & z &= \frac{\bar{z}}{R_0}, & z_0 &= \frac{\bar{z}_0}{R_0}, & t &= \omega_p \bar{t}, & \delta &= \frac{\bar{\delta}}{R_0}, & \tau &= \frac{\bar{\tau}}{A_0 R_0 / 2}, \\ \theta &= \frac{\bar{\tau}_y}{A_0 R_0 / 2}, \\ R(z) &= \bar{R}(\bar{z}) / R_0, & r &= \bar{r} / R_0, & e &= \frac{A_1}{A_0}, & B &= \frac{a_0}{A_0}, & \omega &= \frac{\omega_b}{\omega_p}. \end{aligned} \right\} \quad (9)$$

The non-dimensional momentum equation (4) becomes

$$\alpha^2 \frac{\partial u}{\partial t} = 4(1 + e \cos t) + 4B \cos(\omega t + \phi) + \frac{2}{r} \frac{\partial}{\partial r}(r \tau_{rz}), \quad (10)$$

where  $\alpha^2 = \frac{\omega_p R_0^2}{(\mu / \rho)}$ ,  $\alpha$  is called Womersley frequency parameter. Equation (6) can be written as

$$\left. \begin{aligned} \tau^2 &= \theta^2 + \frac{1}{\sqrt{2}} \left( -\frac{\partial u}{\partial r} \right)^{\frac{1}{2}}, & \text{if } \tau \geq \theta \\ \frac{\partial u}{\partial r} &= 0 & \text{if } \tau \leq \theta \end{aligned} \right\} \quad (11)$$

The boundary conditions (equations 7 and 8) reduce to

$$u = 0 \quad \text{at} \quad r = R(z) \quad (12)$$

$$\tau \text{ is finite at } r = 0 \quad (13)$$

The geometry of the stenosis in non-dimensional form is given as

$$\frac{R(z)}{R_0} = 1 - \frac{\delta}{R_0} \exp\left(-\frac{m^2 \varepsilon^2 z^2}{R_0^2}\right) \quad (14)$$

$\delta$  is the maximum height of the stenosis at the throat and  $m$  is a parametric constant,  $\varepsilon$  denotes the relative length of the constriction (*i.e.*  $\varepsilon = R_0/L_0$ ),  $R(z)$  and  $R_0$  are the radius of the artery with and without stenosis.

### Method of Solution

The velocity  $u$ , the shear stress  $\tau$ , the plug core radius  $R_p$  and plug core velocity  $u_p$  are assumed to possess the following form:

$$u(z, r, t) = u_0(z, r, t) + \alpha^2 u_1(z, r, t) + \dots \quad (15)$$

$$\tau(z, r, t) = \tau_0(z, r, t) + \alpha^2 \tau_1(z, r, t) + \dots \quad (16)$$

$$R_p(z,t) = R_{0p}(z,t) + \alpha^2 R_{1p}(z,t) + \dots \quad (17)$$

$$u_p(z,t) = u_{0p}(z,t) + \alpha^2 u_{1p}(z,t) + \dots \quad (18)$$

where  $\alpha (< 1.0)$  is the pulsatile Reynolds number.

Substituting (15) and (16) in equation (10) and equating the constant terms and  $\alpha^2$  terms we get

$$\frac{\partial}{\partial r}(r\tau_0) = -2r[(1+e \cos t) + B \cos(\omega t + \phi)], \quad (19)$$

$$\frac{\partial u_0}{\partial t} = \frac{2}{r} \frac{\partial}{\partial r}(r\tau_1) \quad (20)$$

Integrating Equation (19) and using the boundary condition (13) we obtain.

$$\tau_0 = -f(t)r, \quad (21)$$

$$\text{where } f(t) = [(1+e \cos t) + B \cos(\omega t + \phi)] \quad (22)$$

Substituting (15) and (16) in (11) we get

$$-\frac{\partial u_0}{\partial r} = 2[\theta + |\tau_0| - 2\sqrt{\theta\tau_0}], \quad (23)$$

$$-\frac{\partial u_1}{\partial r} = 2|\tau_1|[1 - \sqrt{\theta/\tau_0}] \quad (24)$$

Integrating equation (23), using the relation (21) and the boundary condition (12) we obtain

$$u_0 = f(t)R^2 \left[ 1 - (r/R)^2 - \frac{8}{3} \frac{k}{\sqrt{R}} \left\{ 1 - (r/R)^{\frac{3}{2}} \right\} + \frac{2k^2}{R} \left\{ 1 - (r/R) \right\} \right], \quad (25)$$

where  $k^2 = \theta / f(t)$

The plug core velocity  $u_{0p}$  can be obtained from equation (25) as

$$u_{0p} = f(t)R^2 \left[ 1 - (R_{0p}/R)^2 - \frac{8}{3} \frac{k}{\sqrt{R}} \left\{ 1 - (R_{0p}/R)^{\frac{3}{2}} \right\} + \frac{2k^2}{R} \left\{ 1 - (R_{0p}/R) \right\} \right], \quad (26)$$

where  $R_{0p}$  is the first approximation plug core radius. Neglecting the terms of  $o(\alpha^2)$  and higher power of  $\alpha$  in Equation (17)  $R_{0p}$  can be obtained from (21) as

$$R_{0p} = \theta / f(t) \equiv k^2 \quad (27)$$

Similarly the solution for  $\tau_1, u_1, u_{1p}$  can be obtained using Equation (20), (24), and (25) as

$$\tau_1 = \frac{f'(t)R^3}{8} \left[ 2(r/R) - (r/R)^3 - \frac{8}{21\sqrt{R}} \left\{ 7(r/R) - 4(r/R)^{\frac{5}{2}} \right\} \right], \quad (28)$$

$$u_1 = \frac{f'(t)R^4}{16} \left[ (r/R)^4 + 4(r/R)^2 + 3 + \frac{k}{\sqrt{R}} \left\{ \frac{16}{3}(r/R)^2 - \frac{424}{147}(r/R)^{\frac{7}{2}} + \frac{16}{3}(r/R)^{\frac{3}{2}} - \frac{1144}{147} \right\} + \frac{k^2}{R} \left\{ \frac{128}{63}(r/R)^3 - \frac{64}{9}(r/R)^{\frac{3}{2}} + \frac{320}{63} \right\} \right], \quad (29)$$

$$u_1 = \frac{f'(t)R^4}{16} \left[ (R_{0p}/R)^4 + 4(R_{0p}/R)^2 + 3 + \frac{k}{\sqrt{R}} \left\{ \frac{16}{3}(R_{0p}/R)^2 - \frac{424}{147}(R_{0p}/R)^{\frac{7}{2}} + \frac{16}{3}(R_{0p}/R)^{\frac{3}{2}} - \frac{1144}{147} \right\} + \frac{k^2}{R} \left\{ \frac{128}{63}(R_{0p}/R)^3 - \frac{64}{9}(R_{0p}/R)^{\frac{3}{2}} + \frac{320}{63} \right\} \right], \quad (30)$$

Using Equating (15,16), the total velocity distribution and shear stress can be written as

$$u = f(t)R \left[ 1 - (r/R)^2 - \frac{8k}{3\sqrt{R}} \left\{ 1 - (r/R)^{\frac{3}{2}} \right\} + 2 \frac{k^2}{R} \left\{ 1 - (r/R) \right\} + \frac{\alpha^2 R^2 C}{16} (r/R)^4 - 4(r/R)^2 + 3 + \frac{k}{\sqrt{R}} \left\{ \frac{16}{3}(r/R)^2 - \frac{424}{147}(r/R)^{\frac{7}{2}} + \frac{16}{3}(r/R)^{\frac{3}{2}} - \frac{1144}{147} \right\} + \frac{k^2}{R} \left\{ \frac{128}{63}(r/R)^3 - \frac{64}{9}(r/R)^{\frac{3}{2}} + \frac{320}{63} \right\} \right], \quad (31)$$

$$|\tau|_w = f(t)R \left\{ 1 + \frac{\alpha^2 R^2 C}{8} \left( 1 - \frac{8k}{7\sqrt{R}} \right) \right\}, \quad (32)$$

where  $C = f'(t)/f(t)$ .

The volumetric flow rate  $Q$  is given by

$$Q(t) = 4 \int_0^{R(z)} r u(z, r, t) dr \\ = f(t)R^4 \left[ \frac{1}{4} + \frac{4}{7} \frac{k}{\sqrt{R}} + \frac{1}{3} \left( \frac{k}{\sqrt{R}} \right)^2 + \frac{\alpha^2 R^2 C}{16} \left\{ \frac{2}{3} + \frac{120}{77} \frac{k}{\sqrt{R}} + \frac{32}{35} \left( \frac{k}{\sqrt{R}} \right)^2 \right\} \right], \quad (33)$$

From Equation (33) for small  $k/\sqrt{R}$ , we have

$$f(t) = \frac{Q(t)}{4} \left[ \frac{1}{R^4} - \frac{16}{7} \frac{k}{R^{\frac{9}{2}}} + \frac{37436}{147} \frac{k^2}{R^5} + \frac{\alpha^2 C}{4R^2} \left\{ \frac{2}{3} + \frac{120}{77} \frac{k}{\sqrt{R}} + \frac{32}{35} \frac{k^2}{R} \right\} \right] \quad (34)$$

The impedance (resistance to flow),  $\lambda$  is defined as

$$\lambda = (p_1 - p_2) f(t) / Q(t). \quad (35)$$

Integrating equation (34) and using the conditions  $p = p_1$  at  $z = 0$  and  $p = p_2$  at  $z = L$  and equation (35), we have

$$\lambda = \frac{(L - L_0)}{4} \left[ \frac{1}{R_0^4} - \frac{16}{7} \frac{k}{R_0^{9/2}} + \frac{37436}{147} \frac{k^2}{R_0^5} + \frac{\alpha^2 C}{4} \left\{ \frac{2}{3R_0^2} + \frac{120}{77} \frac{k}{R_0^{5/2}} + \frac{32}{35} \frac{k^2}{R_0^3} \right\} \right] \\ + \frac{1}{4} \left[ \frac{1}{R_0^4} \int_d^{d+L_0} \frac{1}{(R/R_0)^4} dz - \frac{16}{7} \frac{k}{R_0^{9/2}} \int_d^{d+L_0} \frac{1}{(R/R_0)^{9/2}} dz + \frac{37436}{147} \frac{k^2}{R_0^5} \int_d^{d+L_0} \frac{1}{(R/R_0)^5} dz \right. \\ \left. + \frac{\alpha^2 C}{4} \left\{ \frac{2}{3R_0^2} \int_d^{d+L_0} \frac{1}{(R/R_0)^2} dz + \frac{120}{77} \frac{k}{R_0^{5/2}} \int_d^{d+L_0} \frac{1}{(R/R_0)^{5/2}} dz + \right. \right. \\ \left. \left. \frac{32}{35} \frac{k^2}{R_0^3} \int_d^{d+L_0} \frac{1}{(R/R_0)^4} dz \right\} \right] \quad (36)$$

The second approximation plug core radius  $R_{1p}$  can be obtained by neglecting the terms with  $\alpha^4$  and the higher power of  $\alpha$  in equation (17) in the following manner.

The shear stress  $|\tau| = (|\tau_0| + \alpha^2 |\tau_1|)$  at  $r = R_p$  is given by

$$[|\tau_0| + \alpha^2 |\tau_1|] = \theta \quad \text{at } r = R_p \quad (37)$$

Using Taylor's series of  $|\tau_0|$  and  $|\tau_1|$  about  $R_{0p}$  and using  $|\tau_0(R_{0p})| = \theta$ , we get

$$R_{1p} = \frac{-|\tau_1(R_{0p})|}{f(t)} \quad (38)$$

from equations (38), (27), and (17),  $R_p$  can be given by

$$R_p = k^2 - \alpha^2 \frac{f'(t)}{f(t)} \frac{R^3}{8} \left[ 2 \left( \frac{k^2}{R} \right) - \left( \frac{k^2}{R} \right)^3 - \frac{8}{21} \frac{k}{\sqrt{R}} \left\{ 7 \left( \frac{k^2}{R} \right) - 4 \left( \frac{k^2}{R} \right)^{\frac{5}{2}} \right\} \right]. \quad (39)$$

The volumetric flow rate  $Q(t)$  with the help of equation (27) and (30) can be written as

$$Q(t) = f(t) R^4 \left[ \frac{1}{4} + \frac{4}{7} (S^*)^{1/2} + \frac{1}{3} S^* + \frac{\alpha^2 R^2 C}{16} \left\{ \frac{2}{3} + \frac{120}{77} (S^*)^{1/2} + \frac{32}{55} S^* \right\} \right] \quad (40)$$

where  $S^* = k^2 / R = \theta / f(t)R$ . It should be notice that in Eq.(40),  $f(t)$ ,  $R$  and  $\theta$  are known terms and  $Q(t)$  is unknown terms to be determined. The flow rate equation for the steady flow is

$$Q_s = R^4 \left[ \frac{1}{4} + \frac{4}{7} (\theta / R)^{1/2} + \frac{1}{3} (\theta / R) \right] \quad (41)$$

## RESULTS AND DISCUSSIONS

For the purpose of examining the validity of the model, the relevant computational work has been performed for a specific case using available experimental data for the various physical parameters encountered in the present analysis.

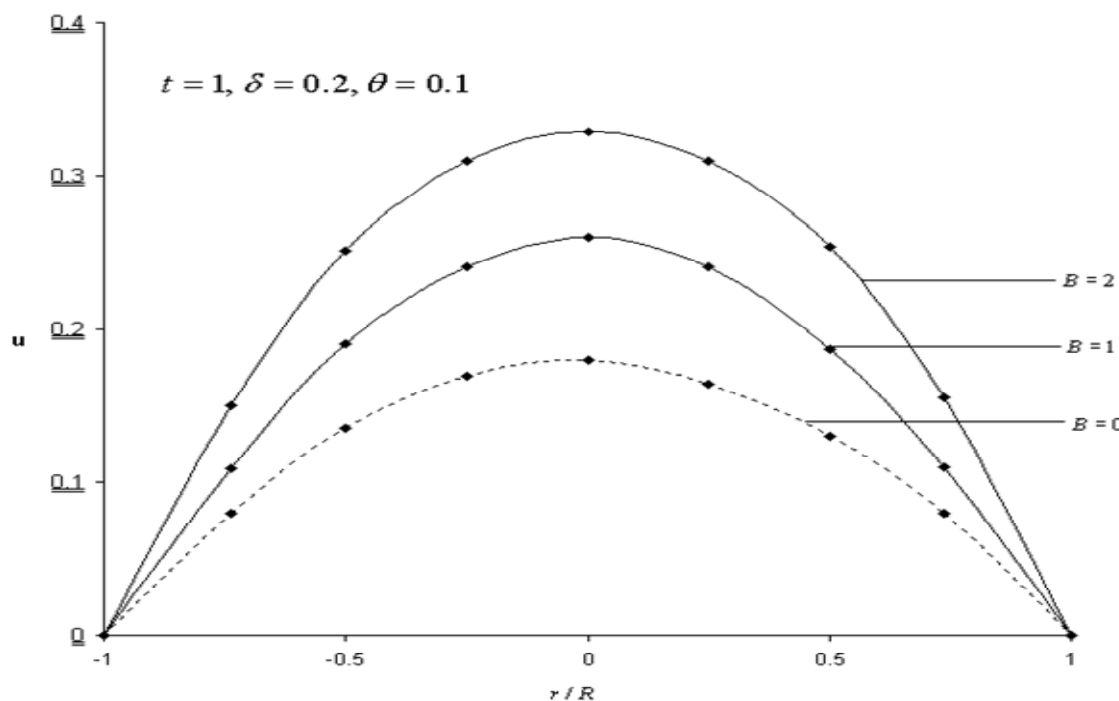


Fig.2. Axial velocity profiles for  $e = 1, \omega = 1, z = 0, \phi = 0.2, \alpha = 0.1$

Figures (2,3,4) illustrates the results for the axial velocity profiles of the streaming blood at the peak of the stenosis for different values of  $B$ ,  $\theta$ ,  $\delta$  and  $t$ . In the presence of body acceleration, velocity increases rapidly. As the body acceleration increases, the plug region shrinks and hence more flow takes place (fig. 2). For a Newtonian fluid (in large blood vessels) velocity rises sharply on the axis of the tube. Increase in yield stress, reduces the velocity as a result of which the plug flow becomes prominent (fig. 3). For a fixed value of yield stress and body acceleration, the axial velocity decreases with time in a stenosed artery (fig. 4). The combined effect of stenosis and yield stress is to enhance the plug flow region.

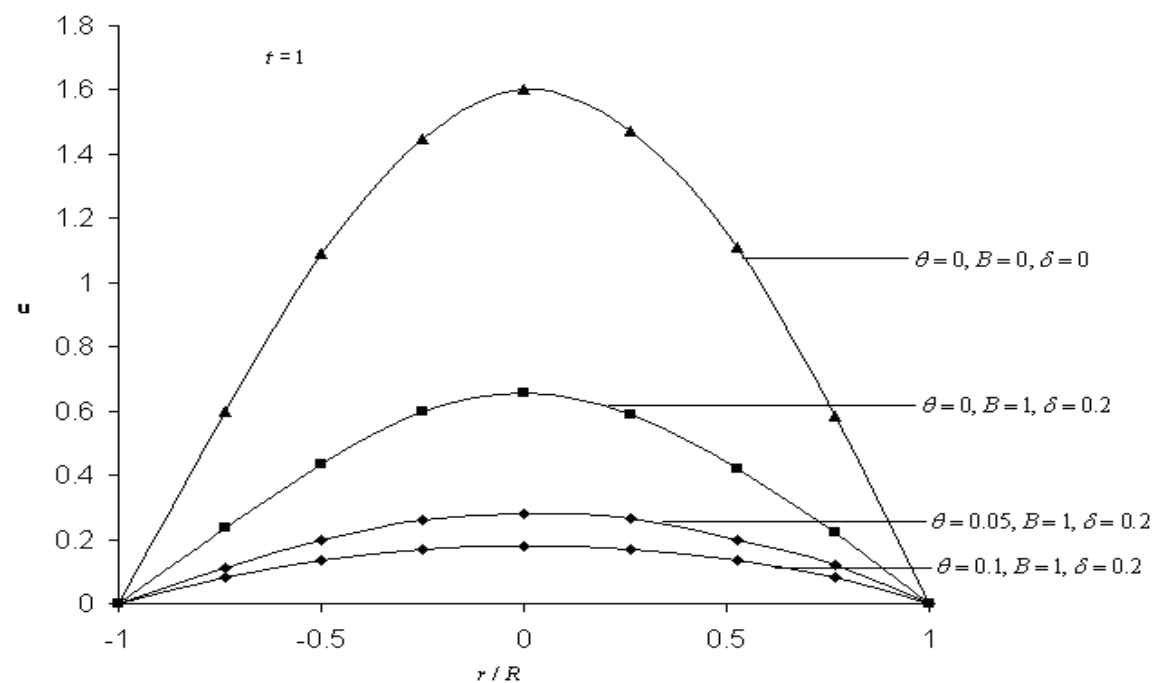


Fig.3. Axial velocity profiles for  $e = 1, \omega = 1, z = 0, \phi = 0.2, \alpha = 0.1$

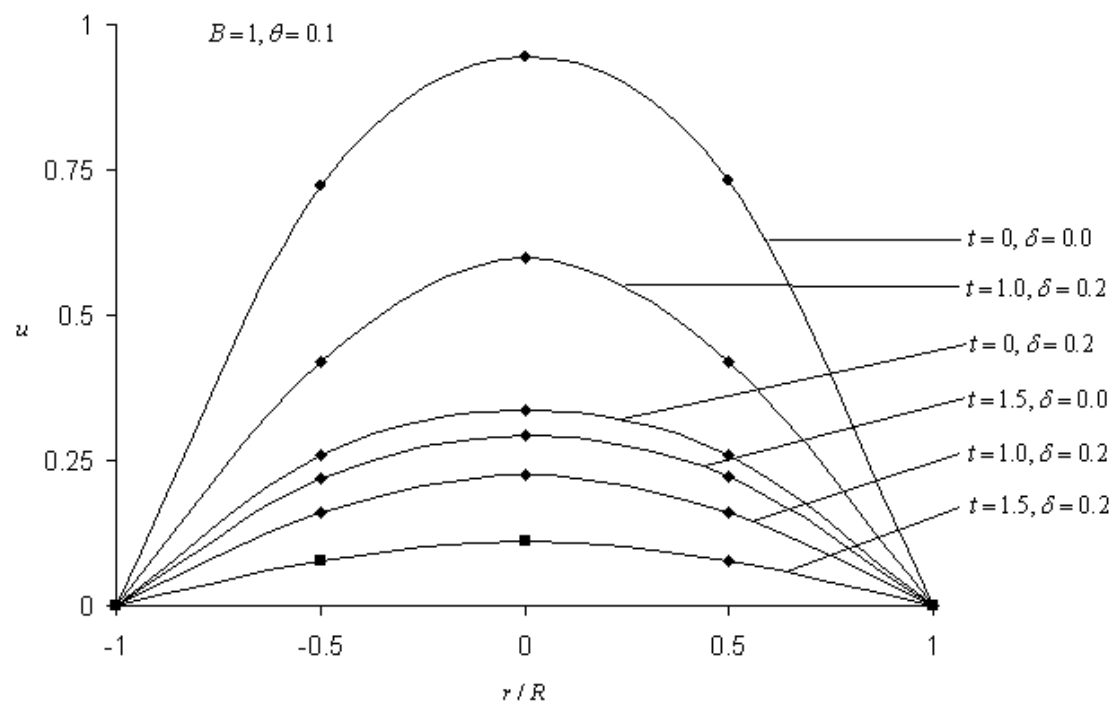


Fig.4. Axial velocity profiles  $e = 1, \omega = 1, z = 0, \phi = 0.2, \alpha = 0.1$

Figure 5 shows the effects of various parameters ( $e$ ,  $\theta$ ,  $B$ ,  $\delta$ ) on the plug core radius. When the body acceleration is not present, in the time cycle, the plug core radius is minimum when  $t = 0^{\circ}$  and it reaches its maximum at  $t = 180^{\circ}$ .

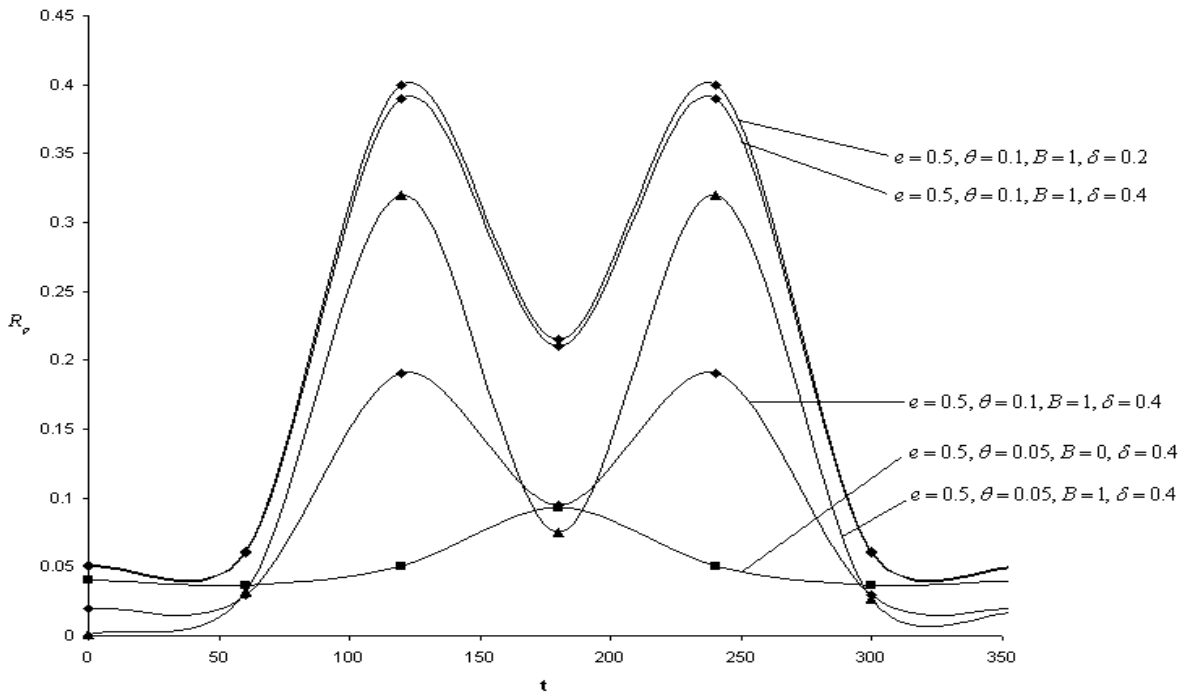


Fig.5. Variation of plug core radius  $R_p$  with time at stenosis throat

In the presence of body acceleration it is seen that plug core radius rises from a minimum value and attains a maximum at  $t = 120^{\circ}$  and then starts decreasing at  $t = 180^{\circ}$ . The same behavior is seen when  $t$  goes from  $t = 180^{\circ}$  to  $t = 360^{\circ}$ .

Figure 6 demonstrates the variation of plug flow velocity for different values of yield stress. In the absence of body acceleration, the plug flow velocity decreases with stenosis height,  $\delta$  and it approaches zero when  $\delta = 0.46$  and in the presence of body acceleration when  $\delta = 0.49$ . It means that for this set of parameters whole region of flow is plugged.

It is clearly depicted from figure. 7 that the plug flow velocity is symmetrical about the time  $t = 180^{\circ}$ . The plug flow velocity is very less in the absence of body acceleration and when  $t$  goes from  $90^{\circ}$  to  $120^{\circ}$  it is more than the corresponding case when body acceleration is present.

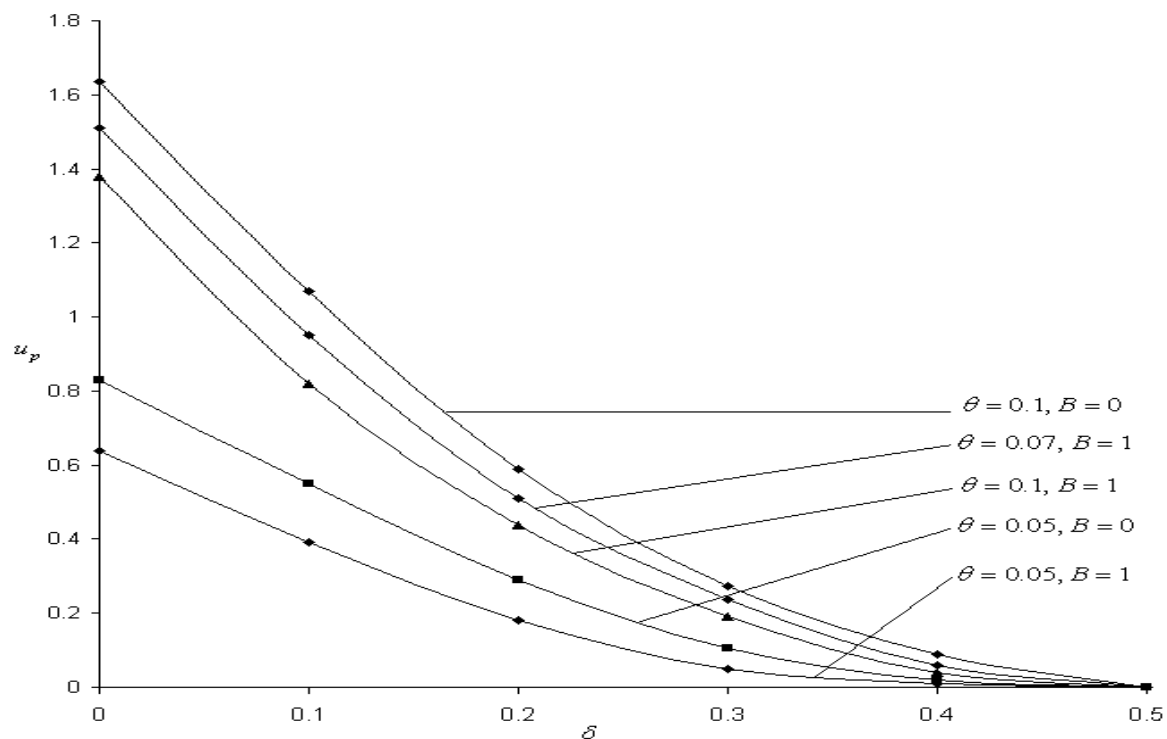


Fig.6. Variation of plug velocity  $u_p$  with stenosis height  $\delta$

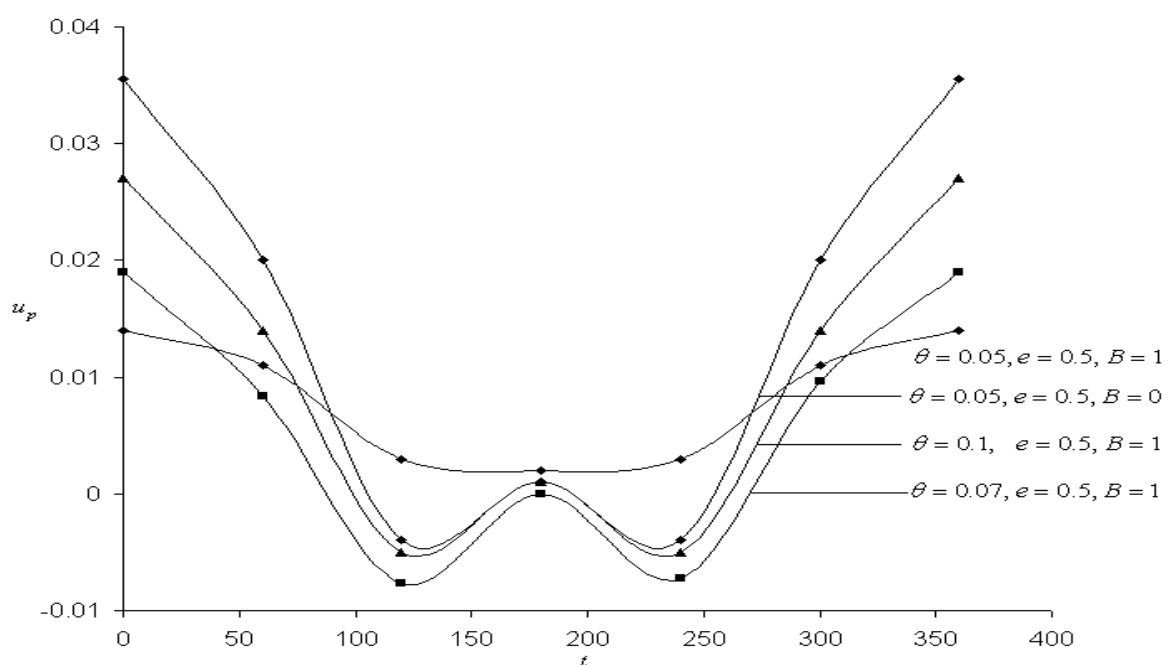


Fig.7. Variation of plug velocity  $u_p$  with time  $t$

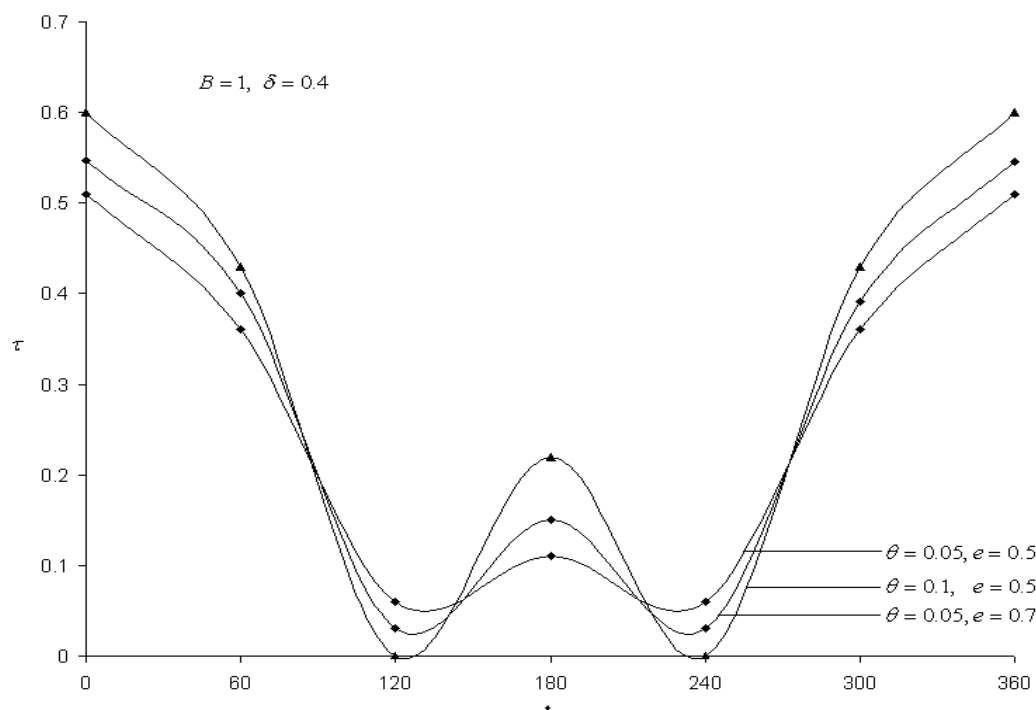


Fig.8. Wall shear stress distribution for different values of  $\theta$  and  $e$

Figures (8, 9) represent the variation of wall shear stress with time  $t$  for different flow parameters ( $e$ ,  $\theta$ ,  $B$ ,  $\delta$ ). At the stenosis throat, the shear stress is symmetrical about  $t = 180^\circ$ . In the absence of body acceleration, one can observe that the wall shear stress is less to the case when body acceleration is present.

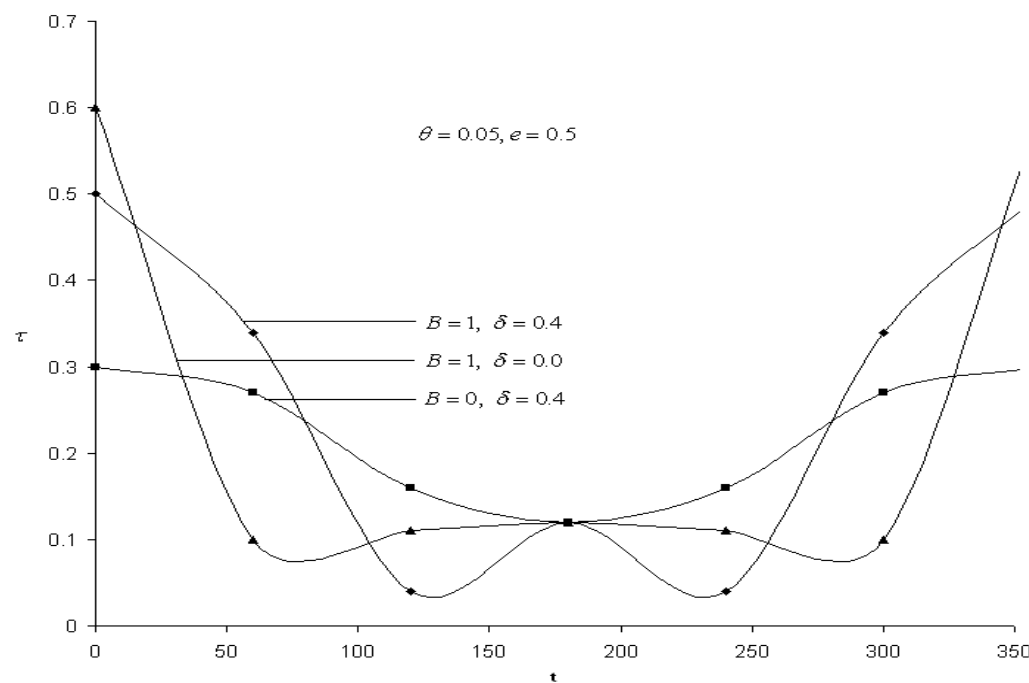


Fig.9. Wall shear stress distribution for different values of  $B$  and  $\delta$

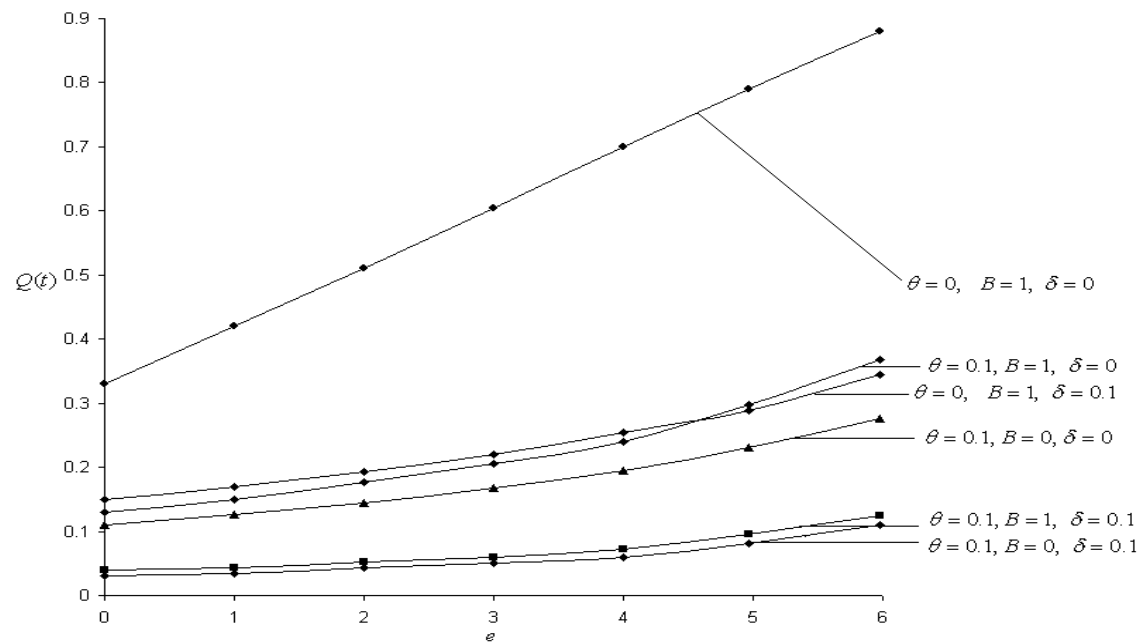


Fig.10. Variation of flow rate  $Q(t)$  with  $e$

The variation of flow rate with pressure gradient is described in figure. 10. For a Newtonian fluid ( $\theta = 0$ ), the curves are linear and when  $\theta$  increases, the curves are slightly non-linear. Flow rate reduces with increasing value of  $\delta$ . It is observed that body acceleration enhances flow rate.

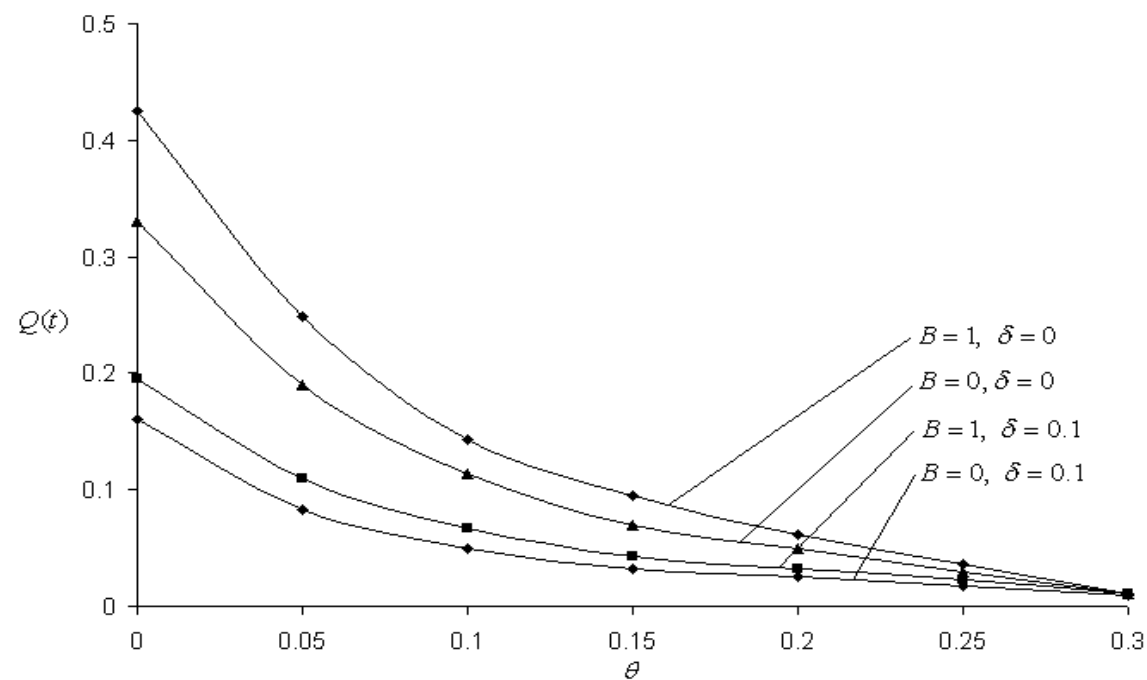


Fig.11. Variation of flow rate  $Q(t)$  with  $\theta$

Figure. 11 reveals the variation of flow rate with yield stress. Increase in  $\theta$  results a substantial decrease in flow rate. This is due to increase in width of plug flow region.

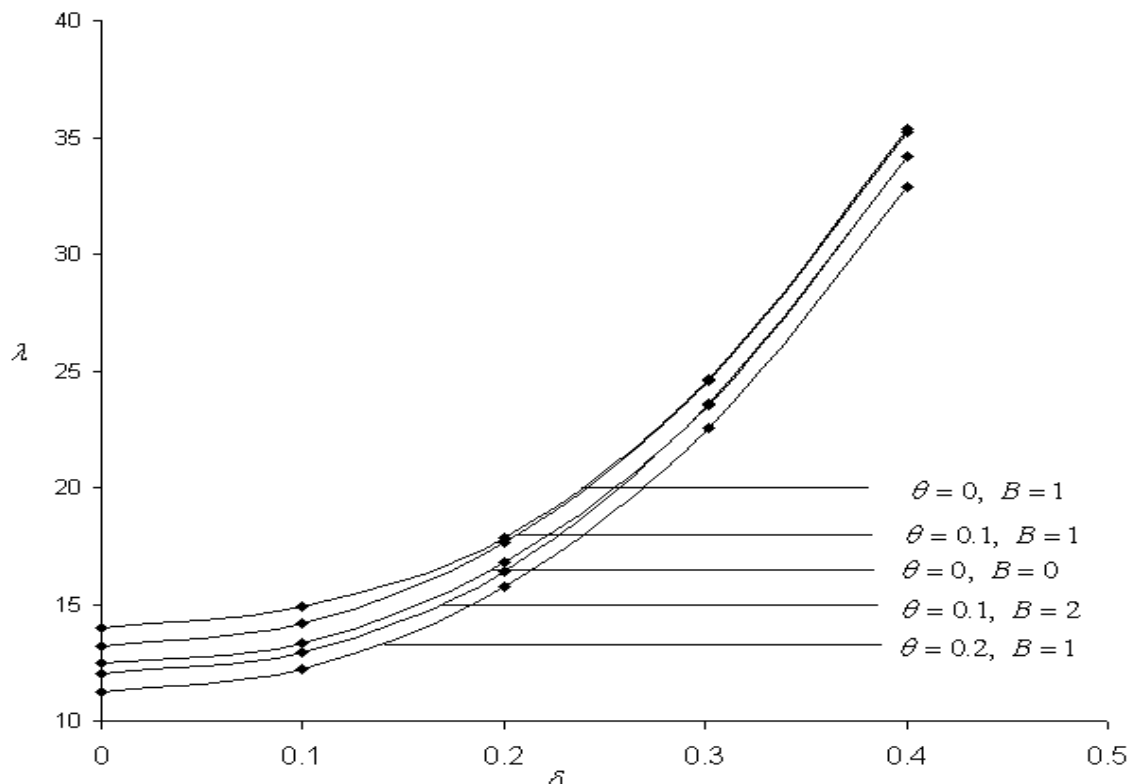


Fig. 12. Variation of flow resistance with stenotic radius  $\delta$

In figure. 12, the variation of the impedance (flow resistance) with the stenosis size has been shown. It is observed that the impedance is highly affected by a small increase in the height of stenosis. In case of a Newtonian fluid ( $\theta = 0$ ), the impedance is very low. In case of non-Newtonian fluid, the yield stress creates more impedance. Hence both the stenosis and yield stress increase the impedance. In the presence of body acceleration, the impedance decreases due to increase in the velocity of fluid.

## CONCLUSION

The present study deals with a theoretical investigation of the characteristics of pulsatile blood flow through a stenosed segment of an artery including the effects of external body acceleration. Blood is represented by Casson (non-Newtonian) fluid model. Using appropriate boundary conditions, analytical expressions for the velocity, yield stress, impedance have been obtained. The yield stress of the fluid and body acceleration highly influenced the velocity of the fluid, shear stress, flow rate and impedance in a stenosed artery. It is interesting to note that the body acceleration enhances the flow rate and reduces the impedance. So this study is more useful for the purpose of simulation and validation of different models in different conditions of arteriosclerosis. This study also provides a scope for estimating the influence of the various parameters mentioned above on different flow characteristics and to ascertain which of the parameters has the most dominating role.

## REFERENCES

1. Belardinelli, E., Ursino, M. and Lemmi, E., "A preliminary theoretical study of arterial pressure perturbations under shock accelerations", ASME J. Biomech. Engg, 111, 233-240, 1989.
2. Charm, S. E. and Kurland, G. S., "Blood Flow and Microcirculation", John Wiley, N. Y. 1964.
3. Cokelet, G.R., "The Rheology of Human Blood: In Biomechanics", Prentice-Hall, Englewood Cliffs, N.J., 1972.
4. El-Shahed, M., "Pulsatile flow of blood through a stenosed porous medium under periodic body acceleration", Appl. Math. Comput., 138, 479-488, 2003.
5. Elshehawey, E.F., Elbarbary, E.M.E., Elsayed, M.E., Afifi, N.A.S. and El-Shahed, M., "Pulsatile flow of blood through a porous medium under periodic body acceleration", Int. J. Theoretical Phys., 39(1), 183-188, 2000.
6. Forrester, J. H. and Young, D.F., "Flow through a converging-diverging tube and its implications in occlusive vascular disease", J. Biomech. 3, 297-316, 1970.
7. Hersey, D., Byrnes, R. E. and Roam, A. M., "Blood Rheology: Temperature dependent of the power-law model", Presented at the A. I. C. H. Meeting, Boston, 1964.
8. Hoogstraten, H., Kootstra, J., Hillen, B., Krijger, J. and Wensing, P., "Numerical simulation of blood flow in an artery with two successive bends," J. Biomech., 29, 1075–1083, 1996.
9. Ishikawa, T., Guimaraes, L. F., Oshima, S. and Yamane, R., "Effect of non-Newtonian property of blood on flow through a stenosed tube," Fluid Dynamics Research, 22, 251–264, 1998.
10. Jung, H., Choi, J. W. and Park, C. G., "Asymmetric flows of non-Newtonian fluids in symmetric stenosed artery," Korea-Aust. Rheo. Journal, 16, 101–108, 2004.
11. Lee, J. S. and Fung, Y. C., "Flow in locally constricted tubes at low Reynolds numbers", J. Appl. Mech. Trans. ASME Ser. E37, 9-16, 1970.
12. Lee, K. and Xu, X., "Modelling of flow and wall behaviour in a mildly stenosed tube," Med. Engg. Phy., 24, 75–586, 2002.
13. Liu, B. and Tang, D., "A numerical simulation of viscous flows in collapsible tubes with stenoses," Appl. Num. Maths., 32, 87–101, 2000.
14. Majhi, S.N. and Nair V.R., "Pulsatile Flow of third grade fluids under body acceleration-modelling blood flow", Int. J. Engg. Sci., 32, 839-846, 1994.
15. Mandal, P.K., Chakravarty, S., Mandal, A. and Amin, N., "Effect of body acceleration on unsteady pulsatile flow of non-Newtonian fluid through a stenosed artery", Appl. Math. Comput., 189, 766-779, 2007.
16. Merrill F.W., Benis, A.M., Gilliland. E.R., Sherwood, T.K. and Salzman, E.W., "Pressure-Flow Relations of Human Blood in Hollow Fibers at Low Flow Rates", J. Appl. Physiol. 20, 954-967. 1965.
17. Migliavacca, F., Dubini, G., Pennati, G., Pietrabissa, R., Fumero, R., Hsia, T Y. and de Leval, M.R., "Computational model of the fluid dynamics in systemic-to-pulmonary shunts," Journal of Biomechanics, 33, 549–557, 2000.
18. Migliavacca, F., Petrini, L., Colombo, M., Auricchio, F. and Pietrabissa, R., "Mechanical behavior of coronary stents investigated through the finite element method," Journal of Biomechanics, 35, 803–811, 2002.
19. Migliavacca, F., Yates, R., Pennati, G., Dubini, G., Fumero, R. and de Leval, M. R., "Calculating blood flow from doppler measurements in the systemic-to-pulmonary

- artery shunt after the norwood operation: a method based on computational fluid dynamics,” *Ultrasound in Medicine and Biology*, 26, 209–219, 2000.
20. Mishra, J. C. and Chakravarty, S., “Flow in arteries in presence of stenosis”, *J. Biomech.* 19, 907-918, 1986.
21. Mishra, J.C. and Sahu, B.K., “Flow through blood vessels under the action of a periodic acceleration field: A mathematical Analysis”, *Comput. Math. Appl.*, 16, 993-1016, 1988.
22. Oshima, M., Torii, R., Kobayashi, T., Taniguchi, N. and Tukagi, K., “Finite element simulation of blood blow in the cerebral artery,” *Computer methods in applied mechanics and engineering*, 191, 661–671, 2001.
23. Redaelli, Boschetti, F. and Inzoli, F., “The assignment of velocity profiles in finite element simulations of pulsatile flow in arteries,” *Computers in Biology and Medicine*, 27, 233–247, 1997.
24. Sarojamma, G. and Nagarani, P., “Pulsatile flow of Casson fluid in a homogeneous porous medium subject to external acceleration”, *Int. J. Non-Linear Differ. Eqns. Theor. Models Appl.*, 7, 50-64, 2002.
25. Siddiqui, S.U. and Mishra, S., “A study of modified casson’s fluid in modelled normal and stenotic capillary- tissue diffusion phenomena”, *Appl. Math. Comput.*, 189, 1048-1057, 2007.
26. Siddiqui, S.U., Gupta, R.S., Verma, N.K. and Mishra, S., “Mathematical Modelling of Pulsatile Flow of Casson’s Fluid in Arterial Stenosis”, *Appl. Math. Comput.*, 210(1), 1-10, 2009.
27. Sud, V.K. and Sekhon, G.S., “Arterial Flow under periodic body acceleration”, *Bull. Math. Biol.*, 47, 35-52, 1985.
28. Taylor, A., Hughes, T. J. and Zarins, C. K., “Finite element modeling of blood flow in arteries,” *Computer methods in applied mechanics and engineering*, 158, 155–196, 1998.
29. Tu, C. and Deville, M., “Pulsatile flow of non-newtonian fluids through arterial stenoses,” *J. Biomech.*, 29, 899–908, 1996.
30. Young, D. F. and Tsai F. Y., “Flow characteristics in models of arterial stenosis – steady flow”, *J. Biomech.*, 6, 395-410, 1973.
31. Young, D. F., “Effects of a time-dependent stenosis of flow through a tube”, *J. Eng. Ind.*, 90, 248-254, 1968.
32. Young, D. F., “Fluid mechanics of arterial stenosis”, *J. Biomech. Eng.*, 101, 157-175, 1979.